New Quantum Invariants of Planar Knotoids

Moltmaker, W.; van der Veen, R.

DOI
10.1007/S00220-023-04738-1

Publication date
2023

Document Version
Final published version

Published in
Communications in Mathematical Physics

Commun. Math. Phys. 402, 695–722 (2023)
Digital Object Identifier (DOI) https://doi.org/10.1007/s00220-023-04738-1

Communications in
Mathematical Physics

New Quantum Invariants of Planar Knotoids

Wout Moltmaker[1], **Roland van der Veen**[2]

[1] Korteweg-de Vries Institute, University of Amsterdam, Science Park, 1098 XG Amsterdam, Noord-Holland, The Netherlands. E-mail: w.c.moltmaker@uva.nl
[2] Bernoulli Institute, University of Groningen, Nijenborgh, 9747 AG Groningen, The Netherlands. E-mail: r.i.van.der.veen@rug.nl

Received: 9 September 2022 / Accepted: 14 April 2023
Published online: 29 May 2023 – © The Author(s) 2023

Abstract: In this paper we discuss the applications of knotoids to modelling knots in open curves and produce new knotoid invariants. We show how invariants of knotoids generally give rise to well-behaved measures of how much an open curve is knotted. We define biframed planar knotoids, and construct new invariants of these objects that can be computed in polynomial time. As an application of these invariants we improve the classification of planar knotoids with up to five crossings by distinguishing two pairs of prime knotoids that were conjectured to be distinct by Goundaroulis et al.

1. Introduction

Knotoids were introduced by Turaev in [21]. Intuitively, a knotoid on a surface Σ is a knot diagram on Σ with two open ends that are allowed to lie in and region of the diagram. This last property is in contrast with long knots or tangles drawn in the plane, who's endpoints must lie in the exterior region. Hence knotoids can be seen as a generalization of long knots. For applications one is usually interested in the cases $\Sigma = S^2$ or $\Sigma = \mathbb{R}^2$, and in this paper we shall focus on these cases. Knotoids on S^2 and $\mathbb{R}^2$ are referred to as **spherical** and **planar**, respectively.

The most prevalent application of knotoids is to the topology of knotted open curves [3,8,9]. Examples of such curves are plentiful in chemistry and molecular biology, see for example [2,5,14,16], but quantifying the knottedness of such a curve remains difficult. The problem is that finding the knottedness of an open curve is not a well-posed problem: while closed curves (knots) fall into different equivalence classes under ambient isotopy (their knot type), all open curves are clearly equivalent under ambient isotopy. In this paper we discuss how the knottedness of open curves can be rigorously quantified, and show that knotoids are a useful tool for doing so. In particular we formalize what it means to quantify the knottedness of an open curve by defining **knot measures**. We then give a large class of examples of such knot measures by showing that every invariant of spherical knotoids produces a knot measure, generalizing the results of [18].

After discussing how invariants of knotoids can be used to extract topological information of open curves, we go on to construct several new invariants of planar knotoids. In particular we define the universal quantum invariant of planar knotoids associated to a given ribbon Hopf algebra. In fact this is an invariant of 'biframed' knotoids, which we introduce and discuss at some length in a preliminary section. We show that all quantum invariants defined in [15] can be recovered from these universal quantum invariants, thereby demonstrating their 'universality'. We then consider the specific example of the Hopf algebra $\mathbb{D}$ introduced in [1], and discuss a computer implementation to compute its universal quantum invariant up to fixed order in a formal power expansion, within polynomial time.

While spherical knotoids are relatively well-understood, being tabulated up to 6 crossings [7], planar knotoids have proven to be more difficult to classify. In [7] a table of prime planar knotoids with up to 5 crossings is produced and it is found that there are between 944 and 950 prime planar knotoids with 5 crossings. (Compare this with the spherical case, where there are only 24 prime knotoids with 5 crossings.) We see that the classification of planar knotoids with 5 crossings is almost complete, with the exception of 6 unresolved pairs of knotoid diagrams that no known invariant of planar knotoids can distinguish but that are nevertheless thought to be in-equivalent. Having defined universal quantum invariants of planar knotoids we consider one such invariant, and show that it can be used to resolve 2 of the 6 unresolved pairs of planar knotoids. We thereby improve on the classification of planar knotoids, and hence on known techniques of distinguishing knotoids.

The outline of this paper is as follows: In Sect. 2 we define the objects of interest to us, namely knotoids, simple theta-curves, H-curves, and biframed planar knotoids. Next, in Sect. 3 we discuss a general framework for how knotoids and knotoid invariants can be applied to quantify the knottedness of open curves. In Sect. 4 we define universal quantum invariants of biframed planar knotoids, relate them to the invariants discussed in [15], and define a new quantum invariant of planar knotoids which can be computed in polynomial time based on [1]. In Sect. 5 we carry out example computations of the new invariant considered in Sect. 4, distinguishing some of the unresolved pairs of planar knotoids from [7].

2. Definitions

In this section we will review the basic objects of study in this paper, namely planar and spherical knotoids, biframed knotoids, and the objects in S^3 whose ambient isotopy classes they are in bijection with.

2.1. Knotoids and geometric realizations

Definition 1 [21]. Let Σ be a surface. A **knotoid diagram** on Σ is a smooth immersion $\phi : [0, 1] \to \Sigma$ whose only singularities are transversal double points away from $\phi(\{0, 1\})$, equipped with over/undercrossing data. For a knotoid diagram ϕ we refer to $\phi(0)$ and $\phi(1)$ as the **leg** and **head** of ϕ, respectively. We say that two knotoid diagrams are **equivalent** if they can be related by a sequence of ambient isotopies and applications of the Reidemeister moves $R1$, $R2$, $R3$ familiar for knot diagrams. A **knotoid** on Σ is an equivalence class of knotoid diagrams on Σ.

Remark 1. We explicitly note that the definition of equivalence of knotoid diagrams does not allow for either of the **forbidden moves** depicted in Fig. 1 that involve a crossing

Fig. 1. The forbidden moves on knotoid diagrams

and an end-point. Indeed, the forbidden moves can clearly be used to render any knotoid trivial.

We stress that knotoids are *diagrams* on Σ, and while they are essentially open-ended knot diagrams they do not correspond to open curves in some 3-manifold in the same way that classical knots correspond to closed curves in S^3. Instead, the class of three-dimensional objects that knotoids on Σ are in one-to-one correspondence with depends on Σ, as we shall see below. In what follows we focus on $\Sigma \in \{\mathbb{R}^2, S^2\}$:

Definition 2. Knotoids on $\mathbb{R}^2$ are called **planar knotoids**, while those on S^2 are referred to as **spherical knotoids**.

We now move on to the description of **geometric realizations** of knotoids, by which we mean sets of objects in three dimensions whose ambient isotopy equivalence classes are in in one-to-one correspondence with knotoids. For example, by Reidemeister's theorem equivalence classes of knot diagrams are in one-to-one correspondence with ambient isotopy classes of knots in S^3. We therefore say that knots form the geometric realization of knot diagrams. In knot theory we generally make no distinction and refer to both objects as knots. With knotoids one has to be slightly more careful, since it turns out that knotoid diagrams are not simply projections of their geometric realizations as is the case for knots. Indeed, if this were so then the geometric realization of knotoids would be open curves in S^3, but all open curves in S^3 are trivial up to ambient isotopy.

Instead, V. Turaev showed that spherical knotoids are in one-to-one correspondence with **simple theta-curves** [21], casting these as the geometric realization of spherical knotoids:

Definition 3. A **theta-curve** is an embedding $\theta : \Theta \to S^3$ into S^3 of the graph Θ that consists of two vertices $\{v_0, v_1\}$ and three edges $\{e_+, e_0, e_-\}$ between them. We say two theta-curves are **equivalent** if they can be related by an ambient isotopy of S^3 that preserves the labels of the vertices and edges of θ. We say a theta-curve is **simple** if $\theta(e_+ \cup e_-)$ is equivalent to the unknot in S^3.

Remark 2. The embeddings $\Theta \hookrightarrow S^3$ defining theta-curves are always assumed to be smooth, in the sense that they are smooth at every point of Θ that has a neighbourhood homeomorphic to $\mathbb{R}$. More generally in the following we assume all embeddings of spaces X into S^3 are smooth at all points where X is locally flat.

A simple theta-curve θ is essentially a knotted open curve, namely $\theta(e_0)$, whose end-points are anchored to an unknotted circle in S^3. This observation forms the intuition for the following result:

Proposition 1. *[21, Thm. 6.2] Equivalence classes of simple theta-curves are in one-to-one bijection with spherical knotoids, i.e. simple theta-curves form the geometric realtization of spherical knotoids.*

In [9], the results from [21] on simple theta-curves were adapted to give a geometric realization of planar knotoids. We adjust their result slightly, working in the thickened plane $\mathbb{R}^2 \times [-1, 1]$ rather than in $\mathbb{R}^3$, and cast this geometric realization in terms of what we shall call **simple H-curves**:

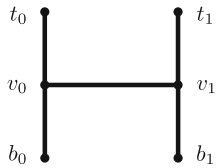

Fig. 2. A drawing of the graph H

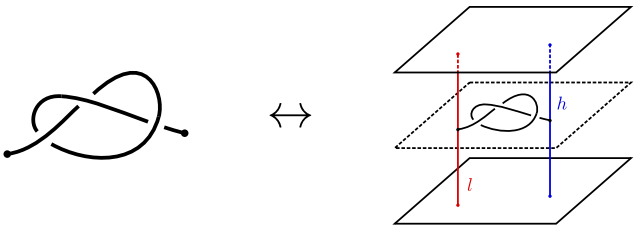

Fig. 3. The bijection used in the proof of Proposition 2

Definition 4. Let H denote the graph with vertex set $\{v_0, v_1, t_0, t_1, b_0, b_1\}$ and edge set $\{(t_i, v_i), (v_i, b_i)\}_{i=0,1} \cup \{(v_0, v_1)\}$; see Fig. 2.

An H-**curve** is an embedding $\phi : H \to \mathbb{R}^2 \times [-1, 1]$ such that $\phi(t_i) \in \mathbb{R}^2 \times \{1\}$ and $\phi(b_i) \in \mathbb{R}^2 \times \{-1\}$ for $i \in \{0, 1\}$. Two H-curves are said to be **equivalent** if they can be related by a label-preserving ambient isotopy. We refer to the lines $\phi((t_i, v_i) \cup (v_i, b_i)) \subseteq \mathbb{R}^2 \times [-1, 1]$ for $i \in \{0, 1\}$ as the **auxiliary lines** of the H-curve ϕ.

We say an H-curve is **simple** if both of the $(1, 1)$-tangles defined by its auxiliary lines are trivial.

Proposition 2. *Simple H-curves form the geometric realization of planar knotoids.*

Proof. (Sketch): The bijection used to prove the proposition is as follows: given a simple H-curve ϕ, apply an ambient isotopy of $\mathbb{R}^2 \times [-1, 1]$ that turns the auxiliary lines into straight lines $\{p\} \times [-1, 1]$ and $\{q\} \times [-1, 1]$ for some $p, q \in \mathbb{R}^2$. Then project the open curve $\phi((v_0, v_1))$ onto $\mathbb{R}^2 \times \{0\}$ while recording over/under-crossing data to obtain a knotoid diagram (making some small deformations in case the projection happens to contain triple points or cusps). Conversely, given a planar knotoid diagram $\phi : I \to \mathbb{R}^2$ we turn it into a simple H-curve by drawing it on the plane $\mathbb{R}^2 \times \{0\}$ inside $\mathbb{R}^2 \times [-1, 1]$, turning the diagram into a smooth embedding of I by removing its double points using deformations in small neighbourhoods of the double points as specified by the over/under-crossing data, and attaching the auxiliary lines $l = \{\varphi(0)\} \times [-1, 1]$ and $h = \{\varphi(1)\} \times [-1, 1]$ to the leg and head respectively.

This process is depicted in Fig. 3. The proof that this indeed describes a well-defined bijection is given in [9]. □

Note Proposition 2 is equivalent to saying that planar knotoids are in bijection with 'rail knotoids', which were defined in [13]. This equivalence between H-curves and rail knotoids is given by replacing $\mathbb{R}^2 \times [-1, 1]$ by $\mathbb{R}^3$ and extending the auxiliary lines to infinite lines in $\mathbb{R}^3$.

2.2. Biframed knotoids As stated in the introduction, the classification of planar knotoids with 5 crossings is complete with the exception of 6 unresolved pairs [7]. In Sect.

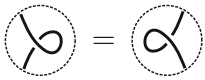

Fig. 4. The weakened first Reidemeister move $R1'$

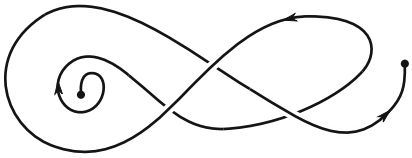

Fig. 5. A biframed knotoid diagram. Here $\boldsymbol{v}$ is taken to point upwards

4 we will construct a new planar knotoid invariant that can distinguish some of these pairs. However this will turn out to be an invariant of 'biframed' knotoids, which were defined in [15]. While [15] focused on biframed spherical knotoids, in this paper we will need to work with biframed *planar* knotoids. In this subsection we define these, and give their geometric realization.

Definition 5 [15]. A **framed knotoid** is an equivalence class of knotoid diagrams under the equivalence generated by the same moves that are allowed for knotoids, but with the first Reidemeister move $R1$ replaced by the **weakened** first Reidemeister move $R1'$, depicted in Fig. 4. The **framing** of a framed knotoid is defined to be the writhe of any of its representative diagrams and is denoted $\mathrm{fr}(K)$.

Definition 6. Fix a vector $\boldsymbol{v}$ on the plane. A **biframed planar knotoid diagram** is a framed planar knotoid diagram $\phi : I \to \mathbb{R}^2$ such that the tangent vectors of ϕ at $0, 1 \in I$ are parallel to $\boldsymbol{v}$. A **biframed planar knotoid** is an equivalence class of biframed planar knotoid diagrams under the equivalence generated by $R1'$, $R2$, $R3$, and ambient isotopies of $\mathbb{R}^2$ that do not change the tangent vector directions of ϕ at $\{0, 1\} \in I$, i.e. smooth deformations of the biframed knotoid diagram such that the resulting diagram at each stage of the deformation is still biframed.

An example of a biframed planar knotoid diagram is given in Fig. 5. Note in this figure that the loop winding around the diagram's starting point cannot easily be removed from the biframed diagram by an allowed isotopy. Indeed, the standard isotopy that achieves this is given by turning the tangent direction at the starting point one full turn to 'unwind' the loop, but this isotopy is not an equivalence of biframed diagrams.

Note that biframed knotoids are in particular framed. To justify the terminology 'biframed' we show that restricting the tangent vectors of a knotoid at its leg and head amounts to attaching another integer to the knotoid.

Definition 7. Let K be a biframed planar knotoid diagram. Then we define the **coframing** of K by

$$\mathrm{cofr}(K) = n_0 - n_1.$$

where n_0 is the winding number of K with respect to the leg and n_1 is the winding number with respect to the head.

The **biframing** of K is defined to be the pair $(\mathrm{fr}(K), \mathrm{cofr}(K))$.

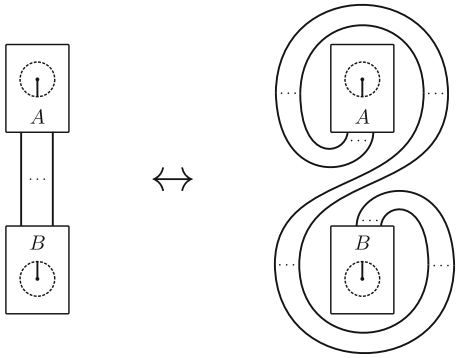

Fig. 6. The 'orbiting' move on a biframed knotoid diagram. Here the boxes labelled A and B are pieces of a knotoid diagram that are identical on both sides of the move, and two parallel strands with dots between them signify any number of parallel strands

In Definition 7 the knotoid diagram K is oriented from leg to head and it should be clear that the winding numbers n_0, n_1 are integers so that the biframing is a pair of integers.

As the terminology suggests, the biframing of a biframed knotoid describes the additional information contained in a biframed knotoid diagram, aside from its knotoid type. This is made precise by Lemma 4 below.

Lemma 3. *The coframing of a biframed planar knotoid is well-defined.*

Proof. Let κ be a diagram of K whose leg and head lie on the same directed line that has the direction of $\boldsymbol{v}$, with the leg coming before the head on this line. As any diagram for K is related to some such κ by an ambient isotopy preserving lines perpendicular to $\boldsymbol{v}$, it suffices to show that $\mathrm{cofr}(K)$ is independent of the chosen diagram κ.

Two choices of κ can clearly be related by applications of $R1'$, $R2$, $R3$, ambient isotopies fixing neighbourhoods of the leg and head, and applications of the 'orbiting' move depicted in Fig. 6 (or its inverse), which is obtained by a full turn of the head of a biframed knotoid around its leg. Thus it suffices to show invariance of $\mathrm{cofr}(K)$ under orbiting moves, as invariance under the others is immediate.

As is shown in Fig. 7, any orbiting move can be reduced to a 'coframing exchange' between the end-points of a biframed knotoid diagram using ambient isotopies fixing neighbourhoods of the leg and head. Invariance of $\mathrm{cofr}(K)$ under coframing exchange on the end-points is immediate, since the loops around the end-points on the right-hand side of Fig. 7 contribute $+1$ and -1 to $\mathrm{cofr}(K)$ respectively. □

Remark 3. From Definition 7 and the proof of Lemma 3 it is clear that biframed knotoids can equivalently be described as knotoid diagrams whose leg and head must lie at fixed points $p, q \in \mathbb{R}^2$ and whose tangent vectors at p, q lie in the direction $q - p$, up to the equivalence generated by $R1'$, $R2$, $R3$, ambient isotopy relative to small neighbourhoods of p, q, and the **coframing identities**, depicted in Fig. 8. This is the perspective on biframed knotoids taken in [15].

Under this approach orbiting moves are no longer allowed, as these are ambient isotopies that move the head or leg of a diagram. So to ensure that Lemma 3 still holds the coframing identities must be imposed separately. This approach has the advantage of reducing the complexity introduced by the coframing to two simple diagrammatic

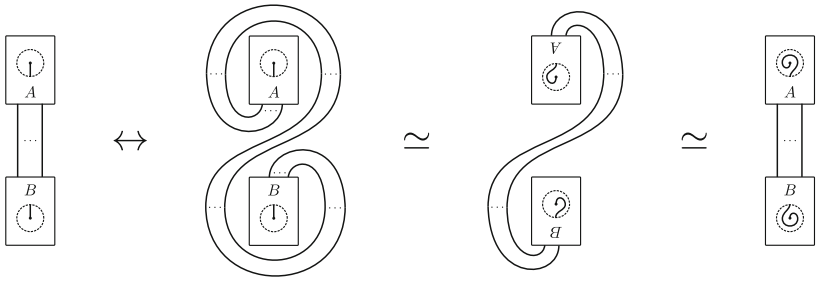

Fig. 7. Sequence of biframed knotoid diagram equivalences showing that an arbitrary orbiting move is equivalent to an coframing exchange (right) on the end-points

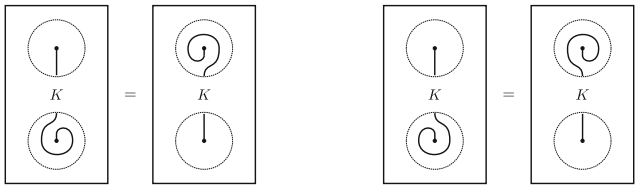

Fig. 8. [15] The coframing identities. Here 'K' denotes the rest of some knotoid diagram that is understood to be identical on both sides of the identities

moves. This can be helpful for proving that some quantity associated to a knotoid diagram is an invariant of biframed knotoids.

Remark 4. The coframing of a biframed knotoid diagram is clearly invariant under crossing changes. Thus generally the easiest way to compute coframing by hand is to apply crossing changes and knotoid diagram equivalences to a diagram until it is a trivial biframed knotoid, for which the coframing can easily be read off from the diagram.

Lemma 4. *There is a bijection*

$$\begin{aligned} \{\textit{Biframed planar knotoids}\} &\leftrightarrow \{\textit{Planar knotoids}\} \times \mathbb{Z}^2 \\ K &\mapsto (K, fr(K), cofr(K)) \,. \end{aligned} \tag{1}$$

Proof. This proof is identical to that of the analogous statement for biframed spherical knotoids, which was given in [15]. □

In subsequent sections we will need to work with explicitly oriented biframed planar knotoids. One caveat with doing so is that, given an oriented biframed knotoid diagram K, its 'reverse' $-K$ is not well-defined. Namely, simply reverting the orientation of such a diagram to obtain $-K$ changes the tangent directions at its endpoints, so that $-K$ is no longer a biframed knotoid diagram. Instead, we define $-K$ as follows:

Definition 8. Let K be an oriented biframed planar knotoid diagram. We define its **reverse** $-K$ to be the biframed planar knotoid diagram given by reversing the orientation of K and adding 'hooks' to the end-points as depicted in Fig. 9 to ensure the tangent vectors of $-K$ at the end-points are in the right direction. The hooks in Fig. 9 are added in such a way that $-K$ has the same coframing as K.

In fact the hooks can also be added in a way opposite to that seen in Fig. 9, by attaching the other end of each hook to the corresponding end-point of $\overline{K}$ instead. This

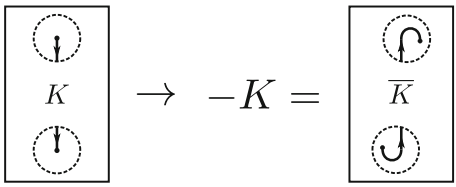

Fig. 9. Definition of $-K$. Here the box labeled 'K' denotes the portion of K that is not pictured, and similarly $\overline{K}$ denotes the diagram K with reversed orientation

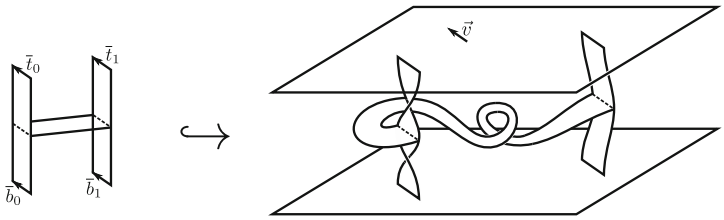

Fig. 10. An embedding of $\overline{H}$ (left) yielding a biframed H-curve (right)

gives another description of $-K$ with coframing equal to that of K. This alternative description is seen to be equivalent to the definition of $-K$ given in Fig. 9 by applying the orbiting isotopy from Fig. 6.

To conclude this section we discuss the geometric realization of biframed planar knotoids. In doing so we will see how coframing, now expressed in terms of winding numbers, indeed corresponds to a framing in the same sense as for framed knots.

Definition 9. Let $\overline{H}$ be the topological space formed by thickening the edges of the graph H depicted in Fig. 2 into three ribbons, as depicted in Fig. 10. Also fix a direction $\boldsymbol{v} \in \mathbb{R}^2$.

A **biframed H-curve** is an embedding of $\overline{H}$ into $\mathbb{R}^2 \times [-1, 1]$ such that the images of the directed line pieces $\bar{t}_0$ and $\bar{t}_1$ depicted in Fig. 10 are line pieces in $\mathbb{R}^2 \times \{1\}$ in the direction of $\boldsymbol{v}$, and the directed line pieces $\bar{b}_0$ and $\bar{b}_1$ are line pieces in $\mathbb{R}^2 \times \{-1\}$ in the direction of $\boldsymbol{v}$.

We say two biframed H-curves A, B are **equivalent** if they can be related by a label-preserving ambient isotopy $F : (\mathbb{R}^2 \times [-1, 1]) \times [0, 1] \to \mathbb{R}^2 \times [-1, 1]$ from A to B such that the embedding $F(-, t) \circ A : \overline{H} \hookrightarrow \mathbb{R}^2 \times [-1, 1]$ defines a biframed H-curve for all $t \in [0, 1]$. This F must be an isotopy from A to B in the sense $F(-, 0) = \mathrm{id}$ so that $F(-, 0) \circ A = A$, and $F(-, 0) \circ A = B$. It must be label-preserving in the sense that the labels on the vertices and edges of $\overline{H}$ are respected.

In analogy with Definition 4, we refer to the images of the vertical ribbons in the depiction of $\overline{H}$ given in Fig. 10 as the **auxiliary ribbons** of a biframed H-curve.

As with biframed planar knotoids, we assign a framing and coframing to biframed H-curves. It suffices to do so for the subclass of 'standard' biframed H-curves, which we define now:

Definition 10. A biframed H-curve A is said to be **standard** if the following conditions hold:

- The framed (1, 1)-tangles corresponding to the auxiliary ribbons of A are trivial- (i.e. unknotted) and unframed (i.e. have framing 0). This is seen for example in Fig. 10, where the auxiliary ribbons are unknotted and have no full twists.

- The auxiliary ribbons of A are in manifestly unframed form, i.e. both are untwisted ribbons of the form $[-\epsilon, \epsilon] \times [-1, 1]$ where $[-\epsilon, \epsilon] \times \{i\}$ lies in $\mathbb{R}^2 \times \{i\}$ along the direction of $\boldsymbol{v}$ for $i \in \{-1, 1\}$.
- Let $\overline{r}$ denote the horizontal ribbon in the depiction of $\overline{H}$ in Fig. 10, and let a_0 and a_1 be its attaching arcs to the vertical ribbons on the left and right, respectively. Then $A(a_i) \subseteq \mathbb{R}^2 \times \{0\}$ for $i \in \{0, 1\}$, and some neighbourhoods in $A(\overline{r})$ of $A(a_0)$ and $A(a_1)$ lie in $\mathbb{R}^2 \times \{0\}$.
- Let r denote one of the horizontal boundary components of $\overline{r}$. Then the tangents to $A(r)$ at $A(a_i)$ are perpendicular to $A(a_i)$ for $i \in \{0, 1\}$.

Definition 11. Let A be a standard biframed H-curve. Parametrize the arc $A(r)$ by $A(r)_t$ for $t \in [0, 1]$ such that $A(r)_i \in A(a_i)$ for $i \in \{0, 1\}$. For $t \in [0, 1]$ we define v_t to be the vector at $A(r)_t$ perpendicular to $A(r)$ pointing into $A(\overline{r})$. Running along $A(r)$ from $A(a_0)$ to $A(a_1)$, the collection $\{v_t\}_{t\in[0,1]}$ defines a path in $SO(2)$, which is a loop by the third assumption in Definition 10. The corresponding element of $\pi_1(SO(2)) \cong \mathbb{Z}$ is defined to be the **framing** of A, and is denoted $\mathrm{fr}(A)$. This number can also be understood as the number of full twists made by the collection $\{v_t\}_{t\in[0,1]}$.

Next consider for all $t \in [0, 1]$ the vectors in $\mathbb{R}^2 \times [-1, 1]$ from $A(r)_0$ and $A(r)_1$ to $A(r)_t$. Project these vectors onto $\mathbb{R}^2 \times \{0\}$ and normalize them. This defines paths p_0 and p_1 in $SO(2)$ as before. If the tangents to $A(r)$ from the fourth assumption in Definition 10 are in the same direction in $\mathbb{R}^2 \times \{0\}$, then these paths are loops. In this case, let n_0 and n_1 be the respective corresponding elements of $\pi_1(SO(2)) \cong \mathbb{Z}$. Then we define the **coframing** of A, denoted $\mathrm{cofr}(A)$, to be

$$\mathrm{cofr}(A) := n_0 - n_1.$$

If the tangents to $A(r)$ from the fourth assumption in Definition 10 have opposite directions, $\mathrm{cofr}(A)$ is not defined. If $\mathrm{cofr}(A)$ is defined, the **biframing** of A is defined to be the ordered pair $(\mathrm{fr}(A), \mathrm{cofr}(A))$.

Remark 5. Note that any biframed H-curve A whose auxiliary ribbons are trivial and unframed $(1, 1)$-tangles can easily be brought into standard form. Note also that the framing and coframing of a standard form of A are independent of the chosen standard form. Indeed, this holds for the framing because the relative twisting between $A(a_0)$ and $A(a_1)$ when transforming an H-curve into standard form is clearly independent of the chosen standard form. The statement for coframing follows from reasoning analogous to the proof of Lemma 3. This observation allows us to define the framing of *any* biframed H-curve A whose auxiliary ribbons are trivial and unframed, namely as that of any standard biframed H-curve equivalent to A. We similarly define the coframing of A to be that of a standard biframed H-curve equivalent to A, if the coframing of the latter is defined.

Finally, we define the objects of interest to us in the context of biframed planar knotoids:

Definition 12. A biframed H-curve A is said to be **simple** if both of the framed $(1, 1)$-tangles defined by its auxiliary ribbons are trivial and unframed, and if the coframing of A is defined.

In particular the biframed H-curve depicted in Fig. 10 is simple, and has biframing $(-1, -1)$.

Theorem 5. *Simple biframed H-curves form the geometric realization of biframed planar knotoids.*

Proof. Let A be a simple biframed H-curve. We can contract the ribbons of $A(\overline{H})$ to obtain a canonical simple H-curve A° from A. We consider the following map:

$$\begin{aligned}\psi : \{\text{Biframed simple } H\text{-curves}\} &\to \{\text{Simple } H\text{-curves}\} \times \mathbb{Z}^2 \\ A &\mapsto \left(A^\circ, \mathrm{fr}(A), \mathrm{cofr}(A)\right).\end{aligned}$$

We claim ψ is a bijection. The proof of this claim is identical to that for the analogous statement for simple biframed theta-curves, see [15]. In short, surjectivity is clear, and for injectivity an equivalence $A^\circ \simeq B^\circ$ easily extends to an equivalence $A \simeq B$ up to framing twists and coframing loops around the auxiliary ribbons, which must cancel if $\mathrm{fr}(A) = \mathrm{fr}(B)$ and $\mathrm{cofr}(A) = \mathrm{cofr}(B)$. This is done e.g. by orbiting moves on the auxiliary ribbons analogous to Fig. 6, but seen as ambient isotopies of $\mathbb{R}^2 \times [-1, 1]$. Combining the bijection ψ with the bijections from Proposition 2 and Lemma 4 we obtain a bijection between biframed simple H-curves and biframed planar knotoids, as required. □

Remark 6. The construction of a spherical knotoids from a planar one by adding ∞ to $\mathbb{R}^2$ corresponds to a map sending biframed H-curves to the biframed theta-curves from [15] as follows: Given a simple biframed H-curve in $\mathbb{R}^2 \times [-1, 1]$ corresponding to a biframed knotoid K, we see it as lying in $\mathbb{R}^3$ and connect the ends of the auxiliary ribbons in the obvious way such that the ribbons form a 0-framed unknotted annulus. The result is a simple biframed theta-curve corresponding to K as a biframed spherical knotoid.

3. Knot Measures

In this section we describe how knotoids and invariants of knotoids can be used to quantify how much a smooth open curve in $\mathbb{R}^3$ is knotted.

The primary application of knotoids to quantifying the knottedness of open curves lies in the observation that projecting an open curve onto a plane typically results in a knotoid diagram. More precisely:

Definition 13. Let C be a smooth open curve in $\mathbb{R}^3$. Then for a direction specified by a vector $\boldsymbol{v}$ on the unit sphere $S^2 \subseteq \mathbb{R}^3$ we define $C_{\boldsymbol{v}}$ to be the diagram given by projecting C onto a plane with normal vector $\boldsymbol{v}$ and recording crossing information.

The procedure of Definition 13 produces a knotoid diagram unless the projection specified by $\boldsymbol{v}$ happens to project an endpoint of the open curve exactly onto one of its strands, or creates cusps or triple points in the diagram. Clearly such problematic projection directions form a measure zero subset of S^2 with respect to the standard measure on the unit sphere $S^2 \subseteq \mathbb{R}^3$, so that we are justified in saying that projecting an open curve 'almost always' results in a knotoid diagram.

The observation motivating Definition 13 also work to produce knot diagrams from closed smooth curves, but by Reidemeister's theorem all knot diagrams $C_{\boldsymbol{v}}$ obtained in this way are equivalent. This is not the case for knotoids: an example of one open curve projecting to two different spherical knotoids is depicted in Fig. 11. This issue stems from the fact that finding knottedness in open curves is an ill-posed problem, since all smooth open curves in $\mathbb{R}^3$ are ambient isotopic.

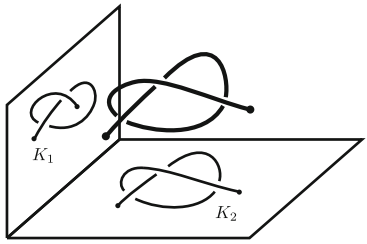

Fig. 11. An open curve projected into different directions, yielding different knotoids K_1 and K_2. The knotoid K_1 is equivalent to the simplest nontrivial spherical knotoid 2_1, while K_2 is equivalent to the trivial knotoid

Knottedness of open curves can therefore not be quantified by an isotopy invariant, as one does for closed curves. Several methods to circumvent this problem have been proposed. The most basic is to reduce to the situation of closed curves by taking a 'statistical closure' or finding the 'dominant knot' in an open curve. This approach is discussed in [6,11,20] for example.

Definition 14. Let C be a smooth open curve in $\mathbb{R}^3$. Place C inside a very large sphere S^2. For every point $\boldsymbol{v} \in S^2$ let $C_{\boldsymbol{v}}$ denote the knot obtained by adding straight lines from the end-points of C to $\boldsymbol{v}$, if this indeed defines a knot. (Like Definition 13, this defines a knot for almost all $\boldsymbol{v} \in S^2$.) We define the **dominant knot** of C to be the knot that has the highest probability of being obtained in this fashion when a point $\boldsymbol{v} \in S^2$ is selected with uniform probability.

The approach of finding a dominant knot is reasonable if our open curve resembles a long knot, but may fail to accurately model the topology of a generic open curve whose endpoints may lie in the middle of a highly tangled region of the curve. Such open curves do not have a canonical closure, and it may not be ideal to model them using a knot. A clear solution to this last objection is instead to work with a 'dominant knotoid':

Definition 15. For a smooth open curve C in $\mathbb{R}^3$ and a vector $\boldsymbol{v}$ on the unit sphere, let $C_{\boldsymbol{v}}$ be as in Definition 13. Then the **dominant knotoid** of C is the knotoid that is most likely to be equivalent to $C_{\boldsymbol{v}}$ when $\boldsymbol{v}$ is selected randomly from S^2 with uniform probability.

While the dominant knotoid of an open curve C may better model the topology of C than its open knot, picking only one of the knotoids arising from an open curve is still somewhat ad hoc. A more uniform approach is taken in [3,8] where S^2 is coloured according to the knotoid type of $C_{\boldsymbol{v}}$ for all $\boldsymbol{v} \in S^2$. While this method is certainly comprehensive in encoding the knottedness of C, it is extremely difficult to implement. Indeed, for certain points $\boldsymbol{v} \in S^2$ the knotoid diagram $C_{\boldsymbol{v}}$ can have a particularly large amount of crossings, making the knotoid type of $C_{\boldsymbol{v}}$ difficult to classify. More-over the classification of knotoids is currently limited: the classification of prime planar knotoids with up to 5 crossings is not yet complete. As a result this method, while very comprehensive, is too difficult to implement for most applications.

A rather different approach is that taken in [18,19], where the knottedness of an open curve C is quantified by a function that depends continuously on the coordinates of C. This is the approach that we further investigate here since it is not particularly ad hoc and will generally result in measures of knottedness that are computable (by virtue of being continuous and hence susceptible to approximation).

In order to generalize the approach taken in [18,19] we define 'knot measures' of open curves. These are meant to be the best thing one can hope for after noting that ambient isotopy invariants cannot detect any information of open curves.

Definition 16. A **knot measure** is a function φ of open curves C taking values in some real vector space, such that:

1. φ is continuous with respect to the topology induced by the Hausdorff metric on the space of images of open curves.
2. There exists a knot invariant $\overline{\varphi}$ that φ extends to in the following sense: As we bring the ends of an open curve C together along a chosen path in the space of open curves to form a knot K, the value of $\varphi(C)$ must converge to $\overline{\varphi}(K)$. As a short-hand:

$$\lim_{C \to K} \varphi(C) = \overline{\varphi}(K).$$

Remark 7. In point 2. of Definition 16, note that C may be closed in several ways to form the same knot K. The limit $\lim_{C\to K} \varphi(C)$ is well-defined by definition, namely by virtue of the ambient isotopy invariance of $\overline{\varphi}$ and hence the independence of $\overline{\varphi}(K)$ from the precise way K is obtained by closing C. Generally, however, the path along which $\varphi(C)$ converges to $\overline{\varphi}(K)$ depends on how C is closed, and $\lim_{C\to K} \varphi(C)$ depends on the knot K that is formed by the chosen closure of C.

In the context of knot measures, the applicability of spherical knotoids to quantifying knottedness of open curves is now expressed by the following theorem:

Theorem 6. *Every spherical knotoid invariant φ gives rise to a knot measure by defining*

$$\varphi(C) := \frac{1}{4\pi} \int_{\boldsymbol{v} \in S^2 - X} \varphi(C_{\boldsymbol{v}})\, dS,$$

on open curves C. Here X is the measure zero subset of S^2 for which $C_{\boldsymbol{v}}$ is not a valid knotoid diagram.

Proof. We check both defining properties of a knot measure, in order:

1. This part of the proof is adapted from [18], where the case in which φ is the Kauffman bracket is discussed. First we restrict to the case where $C = E_n$ lies in the class of polygonal chains consisting of n edges. In this case $(E_n)_{\boldsymbol{v}}$ is one of finitely many knotoids. Let us list these knotoids as $\{K_1, \ldots, K_m\}$. Then

$$\varphi(E_n) = \frac{1}{4\pi} \int_{\boldsymbol{v} \in S^2 - X} \varphi\left((E_n)_{\boldsymbol{v}}\right)\, dS = \sum_{i=1}^{m} p_i \varphi(K_i),$$

   where $p_i = \mathbb{P}\left((E_n)_{\boldsymbol{v}} = K_i\right)$ when $\boldsymbol{v}$ is randomly sampled from $S^2 - X$ with a uniform probability distribution. The proof of [18, Lemma. 3.1] shows that each p_i is a uniformly continuous function of the coordinates of E_n.

Let V be the free vector space over the set $\{\varphi(K_i)\}_{i=1}^m$. Then clearly V is finite-dimensional, namely its dimension is bounded by m. Consider the standard Euclidean norm $\|\cdot\|$ on V. With respect to this norm we have

$$\|\varphi(E_n)\| = \sqrt{\sum_{i=1}^{m} {p_i}^2}.$$

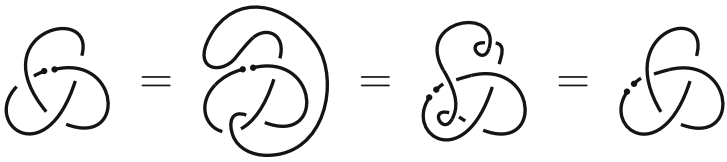

Fig. 12. Showing well-definedness of $K^\bullet$

Thus since each p_i is a uniformly continuous function of the coordinates of E_n we conclude that $\varphi(E_n)$ is too. So the result we wish to prove holds when restricted to the class of polygonal chains with n edges, for any n.

Let $\mathcal{P}$ be the set of all polygonal open chains. If C is any smooth open curve then we can make a sequence of polygonal approximations $\{C_n\}_{n\in\mathbb{N}}$ of C such that for all $\varepsilon > 0$ there exists an $N \in \mathbb{N}$ so that C_n is contained in a tube of radius ε around C for all $n > N$. Thus $\mathcal{P}$ is dense in the space of all open curves. Let W be the vector space over $\mathbb{R}$ spanned by $\{\varphi(K)\}_{K\in\mathcal{K}}$, where $\mathcal{K}$ is the set of all spherical knotoids. Let B be a (Hamel) basis for W contained in $\{\varphi(K)\}_{K\in\mathcal{K}}$. The space W may be infinite-dimensional, but since $\mathcal{K}$ is countably infinite, B is finite or countably infinite. Consider the l^2 norm $\|\cdot\|_2$ on W with respect to B. If W is infinite-dimensional then W is not complete with respect to this norm. However, by construction we have $\|\varphi(C)\|_2 \leq 1$ for all C, so that the image of φ lies inside the copy of l^2 contained in W. Hence we can take the codomain of φ to be complete. By uniform continuity of φ on $\mathcal{P}$, density of $\mathcal{P}$, and completeness of the codomain of φ, we conclude that φ is continuous at C (see, for example, [4, Ch. 24]).

2. This part of the proof follows from canonically associating a spherical knotoid $K^\bullet$ to any knot K [21]. We then define $\overline{\varphi}$ by

$$\overline{\varphi}(K) := \varphi(K^\bullet).$$

The knotoid $K^\bullet$ is defined by taking a diagram of K and removing a small segment from one of its arcs, away from the crossings of K. To see that this is well-defined we must show that $K^\bullet$ is independent of the chosen arc. The proof of this is depicted in Fig. 12: The removed arcs can always be moved over or under one crossing by dragging the obstructing strand of the crossing along the back of S^2 as shown. Note that the proof of this fact also goes through for framed knotoids, since the loops undone by the first Reidemeister move in the last equality of Fig. 12 are oppositely oriented.

Clearly $\overline{\varphi}$ is now a knot invariant, since equivalent knots K and L give rise to equivalent knotoids $K^\bullet$ and $L^\bullet$.

Finally, we prove $\overline{\varphi}$ extends φ. Say that we bring the ends of C together to form a closed curve K. By Reidemeister's theorem all diagrams $K_{\boldsymbol{v}}$ are equivalent to some knot diagram κ. Clearly as the ends of C are brought together, $\mathbb{P}(C_{\boldsymbol{v}} = \kappa^\bullet)$ converges to 1. Hence

$$\lim_{C\to K} \varphi(C) = \frac{1}{4\pi}\int_{\boldsymbol{v}\in S^2-X} \varphi\left(\kappa^\bullet\right)\, dS = \frac{1}{4\pi} 4\pi\varphi(\kappa^\bullet) = \varphi(\kappa^\bullet) = \overline{\varphi}(K),$$

as required. □

Remark 8. The requirement that φ is a *spherical* knotoid invariant is necessary. Namely $K^\bullet$ is not well-defined as a planar knotoid and hence planar invariants φ do not extend to a well-defined knot invariant $\overline{\varphi}$. The fact that $K^\bullet$ is not well-defined as a planar knotoid is

exemplified by the two knotoids at the far left- and right-hand sides of Fig. 12: these are known to be inequivalent as planar knotoids, tabulated in [7] as 3_{16} and 3_1 respectively.

However, for a planar knotoid invariant φ the first part of the proof of Theorem 6 still goes through. So in this case we still obtain a continuous measure of knottedness; just one that doesn't extend to an isotopy invariant on closed curves.

Noting that there is a surjection from planar knotoids to spherical knotoids (induced by the one-point compactification of $\mathbb{R}^2$), we conclude knot measures associated to planar knotoid invariants can generally contain more information about the shape of a knotted open curve than those coming from spherical invariants. However, we see that this information does not have the character of an ambient isotopy invariant, and is therefore of a more geometric nature.

Note that the approach taken in [3,8] where S^2 is colored according to the spherical knotoid type of $C_{\boldsymbol{v}}$ determines the knot measures constructed in Theorem 6. Indeed, after integration over S^2 this approach yields the case of Theorem 6 when φ is the trivially complete knotoid invariant given by

$$\varphi(K) = [\text{Knotoid type of } K].$$

4. Universal Quantum Invariants of Planar Knotoids

In this section we define the universal quantum invariant of biframed knotoids associated to any ribbon Hopf algebra A. We show how all of the quantum invariants of planar knotoids discussed in [15] can be recovered from these universal invariants. Afterwards we follow the approach to universal invariants seen in [1] by working with the algebra $\mathbb{D}$, which is a ribbon Hopf algebra over $\mathbb{Q}[\epsilon][\![\hbar]\!]$ related to quantum $U(\mathfrak{sl}_2)$. In [1] a Mathematica [22] implementation is given for efficiently computing the universal invariant associated to $\mathbb{D}$ up to fixed order in ϵ. We end this section by applying this Mathematica implementation to biframed knotoid diagrams, in order to carry out example computations for universal quantum invariants.

4.1. Universal quantum invariants In this subsection we follow the notation from [17], as all the results for knots that we will generalize to knotoids in this subsection can be found there. Throughout, we assume without loss of generality that the tangent vectors at the endpoints of all biframed planar knotoids are directed vertically downwards, and we let A be a ribbon Hopf algebra. That is, A has morphisms $(m, \Delta, i, \epsilon, S)$ endowing it with the structure of a Hopf algebra, has a quasitriangular structure $\mathcal{R} \in A \otimes A$, and has a central 'ribbon element' v such that

$$\begin{aligned} v^2 &= S(u) \cdot u, \\ \Delta(v) &= (v \otimes v) \cdot (\mathcal{R}_{21}\mathcal{R})^{-1}, \\ S(v) &= v, \\ \epsilon(v) &= 1. \end{aligned}$$

where, writing $\mathcal{R} = \sum_i \alpha_i \otimes \beta_i$, we denote $\mathcal{R}_{21} = \sum_i \beta_i \otimes \alpha_i$ and define $u \in A$ to be given by $u = \sum_i S(\beta_i) \cdot \alpha_i$. Similarly, we will write $\mathcal{R}^{-1} \in A \otimes A$ as a sum of pure tensors using the notation $\mathcal{R}^{-1} = \sum_i \alpha_i' \otimes \beta_i'$.

Given a ribbon Hopf algebra A we will construct an invariant Z_A of oriented biframed planar knotoids, taking values in A, called the 'universal quantum invariant associated

Fig. 13. The elementary knotoid diagram pieces

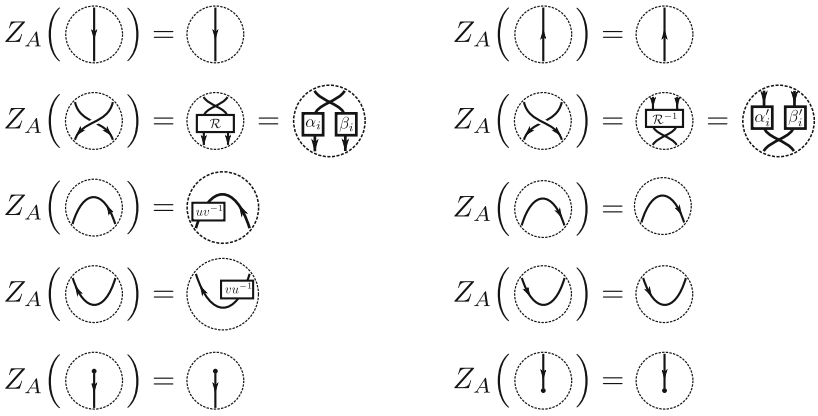

Fig. 14. The value of Z_A on elementary knotoid diagram pieces

to A'. We will describe the construction of this invariant in terms of elementary knotoid diagram pieces.

Definition 17. The **elementary knotoid diagram pieces** are the portions of knotoid diagram depicted in Fig. 13, with either orientation allowed for the unoriented pieces.

Let D_1 and D_2 be tangles, possibly containing the head and/or leg of a knotoid. We define their **tensor product** $D_1 \otimes D_2$ to be their horizontal juxtaposition. If D_1 has n open ends at the bottom and D_2 has n open ends at its top, then we define their **composition** $D_1 \circ D_2$ to be the diagram portion obtained by placing D_1 above D_2 and gluing the open ends at the bottom of D_1 to those at the top of D_2, in order.[1] Note that in this way any biframed knotoid diagram can be decomposed into a finite sequence of compositions and tensor products of elementary knotoid diagram pieces (again, assuming without loss of generality that the tangent vectors at its endpoints are directed vertically downwards).

Definition 18. Let K be an oriented biframed knotoid diagram, and A a ribbon Hopf algebra. We define the **universal quantum invariant** Z_A **associated to** A by decomposing K into compositions and tensor products of elementary knotoid diagram pieces. We evaluate Z_A on these pieces via Fig. 14. We then glue the values of Z_A on these elementary pieces back together by following K. To find $Z_A(K)$ we then run through the resulting diagram from leg to head, multiplying the elements of A placed on K together as we encounter them, and finally sum over all the indices of copies of $\mathcal{R}$ and $\mathcal{R}^{-1}$. The result is an element of A which we define to be $Z_A(K)$.

Example 1. The definition of Z_A is illustrated for an example knotoid in Fig. 15.

[1] This convention for the notation of composition essentially means that we read a composition of diagram portions 'from bottom to top'.

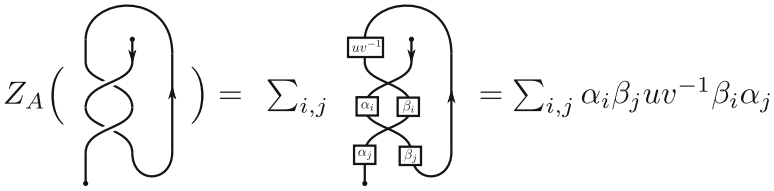

Fig. 15. Computing $Z_A(K)$ for an example knotoid K

Remark 9. In the case of knots, the universal quantum invariant takes values in A/I where I is the vector subspace spanned by elements of the form $xy - yx$ for $x, y \in A$. Namely to compute the universal quantum invariant of knots, one chooses a place to start running through the knot diagram. To ensure the resulting element of A is independent of the chosen starting point, one must therefore quotient by I. This is not the case for knotoids since they, like tangles, have a canonical starting point, namely the leg. If we do consider $Z_A(K)$ as an element of A/I for a knotoid K, then the result is easily seen to be equal to the universal quantum invariant of the virtual closure of K, seen as a rotational virtual knot.[2] See [12] for details on universal quantum invariants of rotational virtual knots.

Lemma 7. *The universal quantum invariant Z_A is an invariant of oriented biframed planar knotoids.*

Proof. By the proof of the analogous statement for framed knots, it suffices to show invariance under the orbiting moves (recall Fig. 6). This is a trivial computation: just evaluate Z_A on all bends and note that every strand obtains exactly two canceling factors uv^{-1} and vu^{-1}. □

The quantum invariant Z_A is 'universal' in the sense that it dominates the quantum invariants defined from a Hopf algebra representation using a Reshetikhin-Turaev construction [15], in analogy with quantum invariants of knots. To show this we first recall the definition of Reshetikhin-Turaev invariants of planar knotoids, phrased in the notation of [17] for consistency.

Definition 19. Let K be an oriented biframed knotoid diagram, A a ribbon Hopf algebra, and (V, ρ) a finite-dimensional representation of A over a field k. Let $R \in \mathrm{End}(V \otimes V)$ and $h \in \mathrm{End}(V)$ be given by

$$R = \tau \circ (\rho \otimes \rho)(\mathcal{R}) \qquad \text{and} \qquad h = \rho(uv^{-1}),$$

where $\tau : x \otimes y \mapsto y \otimes x$. Note that therefore $R(x \otimes y) = \sum_i \rho(\beta_i)(y) \otimes \rho(\alpha_i)(x)$. We further define the morphisms $n : V \otimes V^* \to k, n' : V^* \otimes V \to k, u : k \to V^* \otimes V$, and $u' : k \to V \otimes V^*$ as follows:

$$n(x \otimes f) = f(h(x)), \qquad n'(f \otimes x) = f(x),$$
$$u(1) = \sum_i e^i \otimes h^{-1}(e_i), \qquad u'(1) = \sum_i e_i \otimes e^i,$$

[2] Here the virtual closure is defined by taking a diagram for K such that the direction from its head to its leg is equal to its tangent direction at the end-points, and adding the straight line from head to leg to K interpreting every crossing of this line with K as virtual.

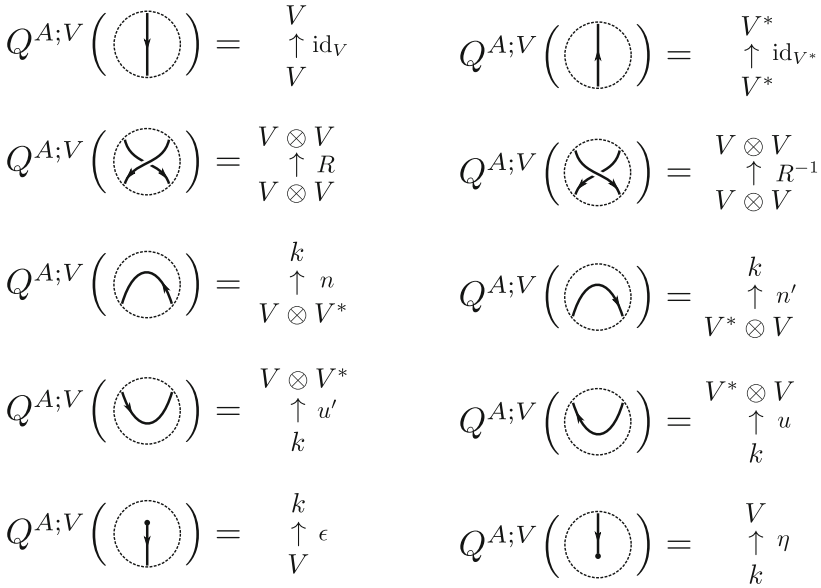

Fig. 16. The value of $Q^{A;V}$ on elementary knotoid diagram pieces

where $\{e_i\}$ is any basis of V and $\{e^i\}$ is the associated dual basis of V^*. Finally, we let $\eta : k \to V$ and $\epsilon : V \to k$ denote the generic linear maps given by $\eta(1) = \sum_i \eta^i e_i$ and $\epsilon(\sum_i \lambda^i e_i) = \sum_i \epsilon_i \lambda^i$ for arbitrary $\{\eta^i, \epsilon_i\} \subseteq k$.

Decompose K into a sequence of compositions and tensor products of elementary knotoid diagram pieces. The **Reshetikhin-Turaev invariant** $Q^{A;V}$ associated to (A, V) is an element of $\mathrm{Hom}(k, k) \cong k$. It is defined by associating the morphisms defined above to elementary knotoid diagram pieces via Fig. 16, and composing the morphisms associated to portions D_1, D_2 of knotoid diagram according to the rules $Q^{A;V}(D_1 \otimes D_2) = Q^{A;V}(D_1) \otimes Q^{A;V}(D_2)$ and $Q^{A;V}(D_1 \circ D_2) = Q^{A;V}(D_1) \circ Q^{A;V}(D_2)$. Note that the result is indeed always an element of $\mathrm{Hom}(k, k)$, since a biframed planar knotoid diagram has no open ends except for its leg and head, which represent morphisms to and from k respectively. See [15,17] for more details.

Lemma 8. *The Reshetikhin-Turaev invariant $Q^{A;V}$ is an invariant of oriented biframed planar knotoids.*

Proof. This can be proven analogously to the proof of Lemma 7. Alternatively, it immediately follows as a corollary from Proposition 9 below. □

Example 2. The definition of $Q^{A;V}$ is illustrated in Fig. 17 for the same example knotoid as Example 1. On the left side of Fig. 17 we sliced the knotoid diagram horizontally along the dotted lines into (tensor products of) the elementary pieces shown in Fig. 16. Reading bottom to top we obtain the composition of maps shown on the right of 17.

$$Q^{A;V}(K) = n \circ (\mathrm{id} \circ \epsilon \otimes \mathrm{id}) \circ (R \otimes \mathrm{id}) \circ (R \otimes \mathrm{id}) \circ (\eta \otimes u').$$

The universality of Z_A means that we can recover $Q^{A;V}$ from Z_A by somehow substituting the representation (V, ρ) of A into Z_A. This is made precise by the following proposition:

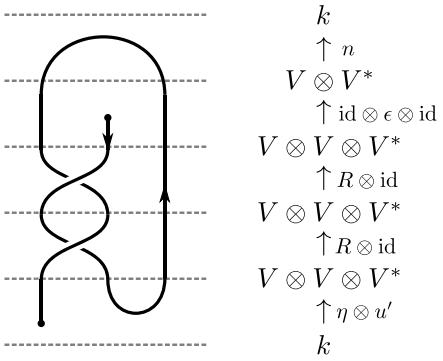

Fig. 17. Computing $Q^{A;V}(K)$ for an example knotoid K

Proposition 9. *Let A be a ribbon Hopf algebra and (V, ρ) a finite-dimensional representation of A. Then for K a biframed knotoid we have*

$$Q^{A;V}(K) = \epsilon \circ \rho\,(Z_A(K)) \circ \eta, \tag{2}$$

where $\eta : k \to V$ and $\epsilon : V \to k$ are the linear maps used in the definition of $Q^{A;V}(K)$.

Proof. This proof is analogous to that for the analogous statement for knots, given in [17]. Let n be the dimension of V. We introduce a state sum formula, and note that it is equal to both sides of Equation (2).

Pick a basis $\{e_i\}$ of V. To construct the state sum we will represent a linear map $f \in \mathrm{Hom}(V^{\otimes n}, V^{\otimes m})$ using tensor notation as $f^{b_1\ldots b_m}_{a_1\ldots a_n}$ so that $f(e_{a_1} \otimes \cdots \otimes e_{a_n}) = \sum_{b_1\ldots b_m} f^{b_1\ldots b_m}_{a_1\ldots a_n} e_{b_1} \otimes \cdots \otimes e_{b_m}$. We represent maps in $\mathrm{Hom}(V^{\otimes n} \otimes (V^*)^{\otimes p}, V^{\otimes m} \otimes (V^*)^{\otimes q})$ similarly using the basis $\{e^i\}$ dual to $\{e_i\}$.

Picking a Morse decomposition for K, we see it as a decorated planar graph with vertices at its crossings and critical points of the vertical coordinate. We associate a label to each of its edges. A state of the diagram K is an association of an element of $\{1, 2, \ldots, n\}$ to every label. We associate a weight $w(E)$ to every elementary knotoid diagram piece via Fig. 18 where, in order to agree with the construction of $Q^{A;V}$ we define

$$n_{ij} := h^j_i, \qquad n'_{ij} := \delta_{ij}, \qquad u^{ij} := (h^{-1})^j_i, \qquad u'^{ij} = \delta_{ij}.$$

We define the state sum of K to be

$$\sum_S \prod_E w(E),$$

where the sum is over all states of K and the product is over all elementary diagram pieces in a decomposition of K into elementary pieces. Now, we have

$$Q^{A;V}(K) = \sum_S \prod_E w(E) = \epsilon \circ \rho\,(Z_A(K)) \circ \eta.$$

Here the first equality follows from expanding the constituents of $Q^{A;V}(K)$ into a sum over indices, and the second equality follows from noting that

$$R^{ij}_{kl} = \sum_m \rho(\alpha_m)^j_k \rho(\beta_m)^i_l \qquad \text{and} \qquad h^i_j = \rho(uv^{-1})^i_j.$$

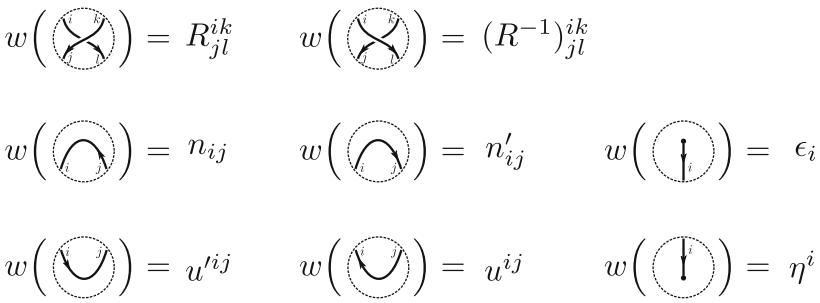

Fig. 18. Weights of the elementary knotoid diagram pieces

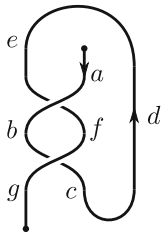

Fig. 19. A generic state of an example knotoid K

See [17, Ch. 4] for further details. □

Example 3. To illustrate the state sum formula from the proof of Proposition 9 we compute it for the same example knotoid as in Examples 1 and 2, and use the result to illustrate the proof of Proposition 9. Label K according to Fig. 19.

Using Fig. 19 we compute

$$\sum_S \prod_E w(E) = \sum R^{ea}_{bf} R^{bf}_{gc} u'^{cd} n_{ed} \epsilon_a \eta^g.$$

Filling in the definitions of R, n, and u', we compute

$$\begin{aligned}
\sum_S \prod_E w(E) &= \sum \sum_{k,l} \rho(\alpha_k)^a_b \rho(\beta_k)^e_f \rho(\alpha_l)^f_g \rho(\beta_l)^b_c \delta_{cd} \rho(uv^{-1})^d_e \epsilon_a \eta^g \\
&= \sum \sum_{k,l} \epsilon_a \rho(\alpha_k)^a_b \rho(\beta_l)^b_c \rho(uv^{-1})^c_e \rho(\beta_k)^e_f \rho(\alpha_l)^f_g \eta^g \\
&= \sum \epsilon_a \ \rho\left(\sum_{k,l} \alpha_k \beta_l u v^{-1} \beta_k \alpha_l \right)^a_g \eta^g \\
&= \sum \epsilon_a \rho(Z_A(K))^a_g \eta^g \\
&= \epsilon \circ \rho\left(Z_A(K)\right) \circ \eta,
\end{aligned}$$

where the fourth equality follows from Example 1. On the other hand, expanding $Q^{A;V}(K)$ from Example 2 into index notation we compute

$$\begin{aligned} Q^{A;V}(K) &= n \circ (\mathrm{id} \circ \epsilon \otimes \mathrm{id}) \circ (R \otimes \mathrm{id}) \circ (R \otimes \mathrm{id}) \circ (\eta \otimes u') \\ &= \sum n_{a_1 a_2} (\mathrm{id} \circ \epsilon \otimes \mathrm{id})^{a_1 a_2}_{b_1 b_2 b_3} (R \otimes \mathrm{id})^{b_1 b_2 b_3}_{c_1 c_2 c_3} (R \otimes \mathrm{id})^{c_1 c_2 c_3}_{d_1 d_2 d_3} (\eta \otimes u')^{d_1 d_2 d_3} \\ &= \sum n_{a_1 a_2} \delta_{a_1 b_1} \epsilon_{b_2} \delta_{a_2 b_3} R^{b_1 b_2}_{c_1 c_2} \delta_{b_3 c_3} R^{c_1 c_2}_{d_1 d_2} \delta_{c_3 d_3} \eta^{d_1} u'^{d_2 d_3} \\ &= \sum n_{b_1 b_3} \epsilon_{b_2} R^{b_1 b_2}_{c_1 c_2} R^{c_1 c_2}_{d_1 d_2} \eta^{d_1} u'^{d_2 b_3} \\ &= \sum_S \prod_E w(E), \end{aligned}$$

where the last equality follows from the change in indices

$$(a, b, c, d, e, f, g) \leftrightarrow (b_2, c_1, d_2, b_3, b_1, c_2, d_1).$$

We conclude this subsection with some results on the behaviour of Z_A under taking the reverse $-K$ of a knotoid K; recall Definition 8.

Lemma 10. *Let K be an oriented biframed planar knotoid. Then $Z_A(-K) = S(Z_A(K))$, where S is the antipode of A.*

This behaviour of Z_A is well-known [1, Thm. 47]. For a proof see e.g. [10]. We note the following result as a corollary:

Corollary 11. *Let K be an oriented biframed planar knotoid. Then $Z_A(K)$ is fixed under S^2, namely $S^2(Z_A(K)) = Z_A(K)$. Similarly $S^{-2}(Z_A(K)) = Z_A(K)$.*

Proof. By Lemma 10 we have that $S^2(Z_A(K)) = Z_A(-(-K))$. From Fig. 9 it is immediate that $-(-K)$ is just K with a +1 coframing loop at its leg and a -1 coframing loop at its head. Thus by Lemma 4 we have that $-(-K) \simeq K$. Therefore the first claim follows since Z_A is a biframed knotoid invariant. The second claim follows immediately from the first. □

4.2. The ribbon Hopf algebra $\mathbb{D}$ Having covered the generalities of quantum invariants of knotoids, we will now introduce a specific ribbon Hopf algebra $\mathbb{D}$ and discuss its associated universal invariant. These are both discussed in [1], where a Mathematica implementation for computing $Z_{\mathbb{D}}$ is also given. After this subsection we use this implementation to compute example values of $Z_{\mathbb{D}}$ for several knotoids; also see Appendix A.

In our discussion only the algebra structure, universal R-matrix, and the ribbon element will be needed.

Definition 20. $\mathbb{D}$ is the algebra over $\mathbb{Q}[\epsilon][\![\hbar]\!]$ generated by $\mathbf{y}, \mathbf{b}, \mathbf{a}, \mathbf{x}$ subject to the relations

$$\begin{aligned} &\mathbf{xy} = e^{\epsilon\hbar}\mathbf{yx} + \frac{1 - e^{-\epsilon\hbar\mathbf{a} - \hbar\mathbf{b}}}{\hbar} \\ &[\mathbf{a}, \mathbf{x}] = \mathbf{x}, \quad [\mathbf{b}, \mathbf{x}] = \epsilon\mathbf{x}, \quad [\mathbf{a}, \mathbf{y}] = -\mathbf{y}, \quad [\mathbf{b}, \mathbf{y}] = -\epsilon\mathbf{y}, \quad [\mathbf{a}, \mathbf{b}] = 0. \end{aligned}$$

Before we can introduce the R-matrix we set $q = e^{\epsilon\hbar}$ and $[k]_q! = \prod_{j=1}^{k} \frac{1-q^k}{1-q}$. Using the Drinfeld double construction it was found in [1] that:

Theorem 12. *$\mathbb{D}$ is a ribbon Hopf algebra with quasitriangular structure*

$$\mathcal{R} = \sum_{m,n=0}^{\infty} \frac{\hbar^{m+n}}{[m]_q!n!} \mathbf{y}^m \mathbf{b}^n \otimes \mathbf{a}^n \mathbf{x}^m$$

and with ribbon element v yielding

$$uv^{-1} = \left(e^{-\epsilon\hbar\mathbf{a}-\hbar\mathbf{b}}\right)^{\frac{1}{2}}.$$

Since $\mathbb{D}$ is ribbon, the techniques of Sect. 4.1 yield a universal quantum invariant of biframed knotoids associated to $\mathbb{D}$.

Remark 10. To discuss the implementation from [1] for computing $Z_{\mathbb{D}}$ we will use the diagrammatic conventions from [1]. This means we will draw our crossings and endpoints directed upwards rather than downwards, from here on.

To get an idea of the strength of $Z_{\mathbb{D}}$ as an invariant of biframed knotoids, we note that $Z_{\mathbb{D}}$ is stronger than all the colored Jones polynomials of biframed knotoids, where the k-th colored Jones polynomial is the Reshetikhin-Turaev invariant associated to $(U_\hbar(\mathfrak{sl}_2), V_k)$. Here $U_\hbar(\mathfrak{sl}_2)$ is the well-known quantum group given by a deformation of the universal enveloping algebra of $\mathfrak{sl}_2$, and V_k is its k-th irreducible representation. To see that $Z_{\mathbb{D}}$ is indeed stronger than the colored Jones polynomials, it suffices to note that $U_\hbar(\mathfrak{sl}_2)$ is isomorphic to a quotient of $\mathbb{D}$. Indeed: it is shown in [1] that setting $\epsilon = 1$ and $\mathbf{t} := \mathbf{b} - \epsilon\mathbf{a} = 0$ in $\mathbb{D}$ yields a ribbon Hopf algebra isomorphic to $U_\hbar(\mathfrak{sl}_2)$.

4.3. Implementation We will briefly describe how the computer program given in [1, App. B] can be used to compute the invariant $Z_{\mathbb{D}}$ for knotoids. The Mathematica implementation can also be found on the second author's website.[3] It carries out computations in $\mathbb{D}$ up to fixed order k in ϵ, with $k = 1$ being sufficient for our purposes.

Say we are given a biframed knotoid diagram K. For simplicity we assume the diagram is upright in that all crossings point upwards. This means the cups and caps come in pairs that either don't contribute to $Z_{\mathbb{D}}$, or that form a full rotation which we call C when it is counter-clockwise and C^{-1} if it is clockwise. Now assign a label to each underpass and overpass of the crossings and also a label to each $C^{\pm}$, making sure no labels appear twice. Denote by $R_{ij}^{\pm}$ the positive/negative crossing with upper strand labeled i and lower strand labeled j. Also denote by $C_i^{\pm}$ any edge rotating (counter)clockwise carrying label i. The knotoid diagram is the result of connecting each crossing and copy of C in the right order, using strands that don't contribute to $Z_{\mathbb{D}}$. We call such a presentation for a knotoid diagram a **rotational tangle decomposition**.

In the program the edges with labels u, v are connected by writing $m_{u,v\to w}$. This produces a longer strand that is now labeled w. Repeating this process for all components $R_{ij}^{\pm}$, $C_i^{\pm}$ in the knotoid diagram yields an expression for $Z_{\mathbb{D}}(K)$ in terms of a multiplication of copies of the values of $R_{ij}^{\pm}$ and $C_i^{\pm}$. The implementation uses efficient expressions of these values as well as of the multiplication $m_{u,v\to w}$ (namely in terms of 'perturbed Gaussian generating functions'; see [1]) to evaluate this expression in $\mathbb{D}$.

A use case for the Mathematica implementation is given in Example 4 below.

Example 4. Say we consider the oriented biframed planar knotoid diagram K depicted in Fig. 20, which is a diagram for the prime planar knotoid tabulated as 5_7 in [7].

[3] http://rolandvdv.nl/PG/.

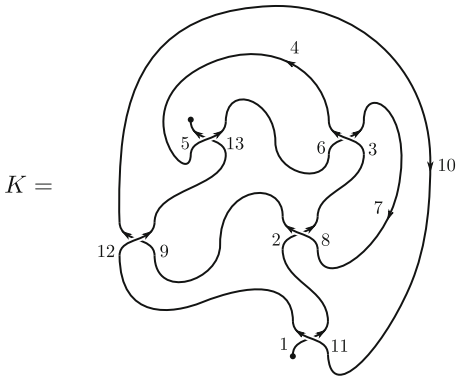

Fig. 20. An oriented biframed planar knotoid diagram K representing 5_7, with labels giving a rotational tangle decomposition of K

The diagram K is drawn so that a rotational tangle decomposition of K is immediately visible. This is indicated by the labels in Fig. 20, representing the labels i, j of copies of $R_{ij}^{\pm}$ and $C_i^{\pm}$ in the diagram. Given this rotational tangle decomposition for the diagram K of 5_7 we can easily read off an expression for $Z_{\mathbb{D}}$ and enter it into Mathematica as follows:

```
In[1]:= Z57 = tR̄11,1 tR12,9 tR̄8,2 tR̄3,6 tR5,13 tC̄10 tC̄7 tC4;
        Do[Z57 = Z57 // tm1,j→1,{j,2,13}];
        PowerExpand[Z57[[3]] // Simplify]
```

Here the first line feeds in the expression for $Z_{\mathbb{D}}(K)$. The second line carries out the multiplication of the elements of $\mathbb{D}$ associated to the rotational tangle components listed in the first line. The third line simplifies the resulting element of $\mathbb{D}$ to a manageable expression.

Running this code will compute $Z_{\mathbb{D}}(K)$ up to the selected order k in ϵ. For our purposes it will suffice to take $k = 1$. The output is then as follows:

$$\text{Out[1]=}\quad \sqrt{T_1}+\frac{-4a_1^2T_1^2+x_1y_1(4+8T_1+4T_1^2-3x_1y_1)-4a_1T_1(-1+T_1+T_1^2+2x_1y_1)}{4T_1^{3/2}}\epsilon+O[\epsilon]^2$$

The invariant we will be particularly interested in is the first-order coefficient of $Z_{\mathbb{D}}(K)$ in ϵ. To obtain this invariant immediately we can alternatively run the following code:

```
In[2]:= Z57 = tR̄11,1 tR12,9 tR̄8,2 tR̄3,6 tR5,13 tC̄10 tC̄7 tC4;
        Do[Z57 = Z57 // tm1,j→1,{j,2,13}];
        Coefficient[PowerExpand[Z57[[3]] // Simplify], ϵ, 1]
```

$$\text{Out[2]=}\quad \frac{-4a_1^2T_1^2+x_1y_1(4+8T_1+4T_1^2-3x_1y_1)-4a_1T_1(-1+T_1+T_1^2+2x_1y_1)}{4T_1^{3/2}}$$

Now let $-K$ be the reverse biframed diagram of the diagram in Fig. 20. By Lemma 10, to compute $Z_{\mathbb{D}}(-K)$ we can apply S to the result of computing $Z_{\mathbb{D}}(K)$. In Mathematica this is done as follows:

```
In[3]:= Do[Z57op = Z57 // tS1, 1];
        Coefficient[PowerExpand[Z57op[[3]] // Simplify], ϵ, 1]
```

Table 1. Unresolved pairs (K_1, K_2) of 5-crossing prime planar knotoids from [7] and their oriented Gauss codes

K_1	K_2	Oriented Gauss code
5_7	5_{421}	-1 -2 3 4 -3 2 -5 1 5 -4 - - - + +
5_9	5_{561}	-1 2 -3 1 -4 5 -2 3 4 -5 - - - + +
5_{12}	5_{593}	-1 2 -3 1 4 -5 -2 3 -4 5 - - - - -
5_{19}	5_{796}	-1 2 -3 4 -5 1 -2 3 5 -4 - - - + +
5_{21}	5_{814}	-1 2 -3 4 -5 1 5 -2 -4 3 - + - - +
5_{24}	5_{891}	-1 2 -3 4 5 -4 -2 1 3 -5 - - - - +

$$\text{Out[3]=} \; -\frac{4(2+a_1)T_1^3+4T_1^2(a_1+a_1^2-x_1y_1)+x_1y_1(-4+3x_1y_1)+T_1(-8(1+x_1y_1)+a_1(-4+8x_1y_1))}{4T_1^{3/2}}$$

Finally, we have mentioned earlier that this Mathematica implementation for computing $Z_{\mathbb{D}}$ is *efficient*. Namely, the following is immediate from [1, Thm. 50]:

Corollary 13. *For K a biframed planar knotoid diagram, one can compute $Z_{\mathbb{D}}(K)$ up to order k in ϵ within $\mathcal{O}(n^{2k+2}\log(n))$ integer operations.*

We conclude orders of ϵ in $Z_{\mathbb{D}}$ are computable in polynomial time for all knotoids, and the Mathematica implementation realizes this [1].

5. Examples

In this section we will refer to specific planar knotoids by using the labels with which they appear in the planar knotoid table given in [7]. For example, 5_7 refers to the 7-th prime knotoid with 5 crossings listed in that table. Table 1 lists the pairs (K_1, K_2) of prime planar knotoids with 5 crossings for which it is conjectured in [7] that $K_1 \not\simeq K_2$.

If all of these pairs were resolved, i.e. shown to be equivalent or distinguished by some invariant of planar knotoids, the classification of prime planar knotoids with up to 5 crossings would be complete. These pairs are particularly difficult to distinguish as they are all equivalent as spherical knotoids (recall any planar knotoid defines a spherical knotoid by adding $\{\infty\}$ to $\mathbb{R}^2$). This follows because they have diagrams with the same oriented Gauss codes, listed in Table 1; see [7] for details. We claim that $Z_{\mathbb{D}}$ can distinguish two of these pairs. Specifically:

Theorem 14. *The universal quantum invariant $Z_{\mathbb{D}}$ of oriented biframed planar knotoids can be used to distinguish the pairs $(5_9, 5_{561})$ and $(5_{12}, 5_{593})$ of planar knotoids.*

Proof. Our strategy is as follows: first we represent the pairs (K_1, K_2) by oriented biframed knotoid diagrams D_1 and D_2 with equal biframing. We will let $-D_1$ denote the diagram resulting from reversing the orientation of D_1. We will then use the computer implementation of $Z_{\mathbb{D}}$ from Sect. 4.3 to compute $Z_{\mathbb{D}}(D_1)$, $Z_{\mathbb{D}}(-D_1)$, and $Z_{\mathbb{D}}(D_2)$ up to first order in ϵ. We shall see that $Z_{\mathbb{D}}(D_1) \neq Z_{\mathbb{D}}(D_2)$ and $Z_{\mathbb{D}}(-D_1) \neq Z_{\mathbb{D}}(D_2)$. Hence $D_1 \not\simeq D_2$ as unoriented biframed knotoids. Since D_1 and D_2 were chosen to have equal biframing and $-D_1$ also has biframing equal to that of D_1, this implies $K_1 \not\simeq K_2$ by Lemma 4.

We now describe the pairs (D_1, D_2) and compute the associated values of $Z_{\mathbb{D}}$ in Appendix A.

Oriented diagrams for 5_9 and 5_{561} are given in Fig. 21. These diagrams are drawn to have equal biframing, as required by the proof strategy outlined above. Note that these

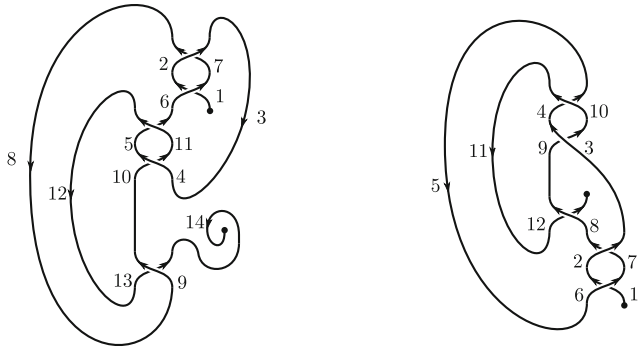

Fig. 21. Biframed planar knotoid diagrams for 5_9 (left) and 5_{561} (right)

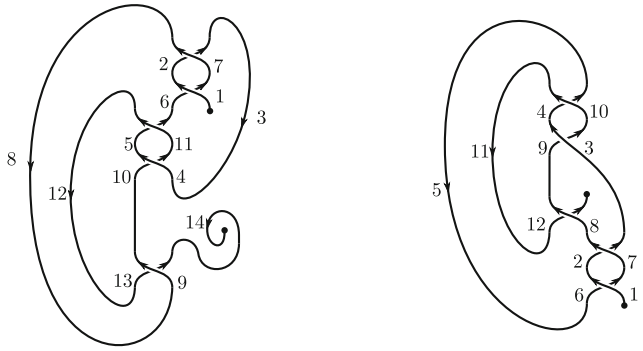

Fig. 22. Biframed planar knotoid diagrams for 5_{12} (left) and 5_{593}

diagrams for 5_9 and 5_{561} can be related to those given in [7] by planar isotopy, as can be checked using the extended Gauss codes of the diagrams, for example.

To see that the diagrams in Fig. 21 indeed have equal biframings, one can compute the writhe of both diagrams to conclude they both have framing -1, and use Remark 4 to find both have coframing -1. Diagrams for 5_{12} and 5_{593} can be obtained by replacing the positive crossings in Fig. 21 by negative ones; see Fig. 22. These diagrams both have biframing $(-5, -1)$ as can be checked by the methods mentioned above.

Now that we have diagrams for all the knotoids under consideration we would like to compute $Z_{\mathbb{D}}$ for these diagrams. To do so we have purposefully drawn them so that their rotational tangle decompositions can be read of immediately, as indicated by the labels in Figs. 21 and 22. We therefore find the following decompositions for these diagrams:

$$
\begin{aligned}
5_9 &= R_{6,1}\, R_{2,7}\, \overline{C}_3\, \overline{R}_{11,5}\, \overline{R}_{4,10}\, C_8\, \overline{R}_{9,13}\, C_{12}\, C_{14},\\
5_{12} &= \overline{R}_{6,1}\, \overline{R}_{2,7}\, \overline{C}_3\, \overline{R}_{11,5}\, \overline{R}_{4,10}\, C_8\, \overline{R}_{9,13}\, C_{12}\, C_{14},\\
5_{561} &= R_{6,1}\, R_{2,7}\, \overline{R}_{3,9}\, \overline{R}_{10,4}\, C_5\, \overline{R}_{8,12}\, C_{11},\\
5_{593} &= \overline{R}_{6,1}\, \overline{R}_{2,7}\, \overline{R}_{3,9}\, \overline{R}_{10,4}\, C_5\, \overline{R}_{8,12}\, C_{11}.
\end{aligned}
$$

By way of a slight abuse of notation, in these decompositions we have used 5_9 to denote the diagram for 5_9 in Fig. 21, and similarly for the other diagrams.

Armed with the decompositions above, it is a simple matter of rerunning the steps of Example 4 to perform the necessary computations of $Z_{\mathbb{D}}$. These computations are

given in Appendix A, where the first orders in ϵ are given for $Z_{\mathbb{D}}(D_1)$, $Z_{\mathbb{D}}(-D_1)$, and $Z_{\mathbb{D}}(D_2)$. Here (D_1, D_2) are either $(5_9, 5_{561})$ or $(5_{12}, 5_{593})$. The results in Appendix A show that in both cases, $Z_{\mathbb{D}}(D_1) \neq Z_{\mathbb{D}}(D_2)$ and $Z_{\mathbb{D}}(-D_1) \neq Z_{\mathbb{D}}(D_2)$ up to first order in ϵ, meaning that $Z_{\mathbb{D}}(D_1) \neq Z_{\mathbb{D}}(D_2)$ and $Z_{\mathbb{D}}(-D_1) \neq Z_{\mathbb{D}}(D_2)$ as required. This finishes the proof of Theorem 14. □

Since both pairs of biframed planar knotoids in Theorem 14 are distinguished by $Z_{\mathbb{D}}$ but equivalent as spherical knotoids, we conclude the following from Theorem 14:

Corollary 15. *$Z_{\mathbb{D}}$ is not an invariant of biframed spherical knotoids, which were defined in [15].*

However, Z_A is an invariant of spherical biframed knotoids and even framed knotoids under certain conditions on the ribbon Hopf algebra A:

Lemma 16. *If $uv^{-1} \in A$ is self-inverse, i.e. $(uv^{-1})^2 = 1 \in A$, then Z_A is an invariant of spherical biframed knotoids. If $uv^{-1} = 1$ then Z_A is in invariant of framed spherical knotoids, which were also defined in [15].*

Proof. The first statement is immediate, since two equivalent biframed spherical knotoids can be related by a sequence of moves of biframed planar knotoids and moves replacing a rotational tangle component C by $\overline{C}$ or vice versa. See [15] for details. The second statement follows from noting that 1 is obviously self-inverse, and that we can adjust the coframing of a biframed knotoid diagram K by adding a number of rotational tangle components C or $\overline{C}$ at either endpoint. Since Z_A associates $1 \in A$ to these components, $Z_A(K)$ is clearly independent of the chosen coframing of K. □

Note that an example where $uv^{-1} = 1$ was already examined in [15]. If $uv^{-1} \neq 1$ then there is a nontrivial contribution to Z_A from coframing loops around the endpoints, causing Z_A to be an invariant of biframed, rather than framed, knotoids.

Acknowledgements. The first author would like to thank Jo Ellis-Monaghan for her guidance, and Kenzo Yasaka and Daniel Boutros for helpful conversations. Both authors express their gratitude to the referees for their comments and suggestions.

Data Availability All data generated or analysed during this study are included in this published article. The Mathematica code used to generate this data is also available on the second author's website http://rolandvdv.nl/PG/ or in [1].

Declarations

Conflict of interest The authors have no relevant financial or non-financial interests to disclose.

A. Mathematica Computations

Below are the computations needed for the proof of Theorem 14, implemented in Mathematica using the code provided in [1, App. B]. The implementation can also be found on the second author's website. In the results of these computations we use the notation $T = e^{-\hbar(\mathbf{b}-\epsilon\mathbf{a})}$. For completeness, our calculations on $(5_7, 5_{421})$ are also included. Note that our calculations show $Z_{\mathbb{D}}(5_7) = Z_{\mathbb{D}}(5_{421})$ up to first order in ϵ, meaning we **cannot** distinguish this pair using the methods described in Sect. 5.

5_7 and 5_{421}:

```
In[4]:= Z57 = tR11,1 tR12,9 tR8,2 tR3,6 tR5,13 tC10 tC7 tC4;
        Do[Z57 = Z57 // tm1,j→1,{j,2,13}];
        Coefficient[PowerExpand[Z57[[3]] // Simplify], ϵ, 1]
```

$$\text{Out[4]}= \frac{-4a_1^2T_1^2+x_1y_1(4+8T_1+4T_1^2-3x_1y_1)-4a_1T_1(-1+T_1+T_1^2+2x_1y_1)}{4T_1^{3/2}}$$

```
In[5]:= Do[Z57op = Z57 // tS1, 1];
        Coefficient[PowerExpand[Z57op[[3]] // Simplify], ϵ, 1]
```

$$\text{Out[5]}= -\frac{4(2+a_1)T_1^3+4T_1^2(a_1+a_1^2-x_1y_1)+x_1y_1(-4+3x_1y_1)+T_1(-8(1+x_1y_1)+a_1(-4+8x_1y_1))}{4T_1^{3/2}}$$

```
In[6]:= Z5421 = tR9,1 tR2,5 tR3,13 tR6,12 tR10,7 tC11 tC8 tC4;
        Do[Z5421 = Z5421 // tm1,j→1,{j,2,13}];
        Coefficient[PowerExpand[Z5421[[3]] // Simplify], ϵ, 1]
```

$$\text{Out[6]}= \frac{-4a_1^2T_1^2+x_1y_1(4+8T_1+4T_1^2-3x_1y_1)-4a_1T_1(-1+T_1+T_1^2+2x_1y_1)}{4T_1^{3/2}}$$

5_9 and 5_{561}:

```
In[7]:= Z59 = tR6,1 tR2,7 tR11,5 tR4,10 tR9,13 tC3 tC12 tC8 tC14;
        Do[Z59 = Z59 // tm1,j→1,{j,2,?}];
        Coefficient[PowerExpand[Z59[[3]] // Simplify], ϵ, 1]
```

$$\text{Out[7]}= 4+2a_1+x_1y_1-x_1^2y_1^2-\frac{x_1y_1(1+x_1y_1)}{T_1^2}+T_1^2(2+x_1y_1+a_1(1+x_1y_1))$$
$$-\frac{8+4x_1y_1-x_1^2y_1^2+4a_1(1+x_1y_1)}{4T_1}-T_1(4+a_1^2+3x_1y_1+2a_1(2+x_1y_1))$$

```
In[8]:= Do[Z59op = Z59 // tS1, 1];
        Coefficient[PowerExpand[Z59op[[3]] // Simplify], ϵ, 1]
```

$$\text{Out[8]}= -a_1^2+\frac{a_1(-1+2T_1-x_1y_1-2T_1^2(1+x_1y_1)+T_1^3(1+x_1y_1))}{T_1^2}$$
$$-\frac{x_1y_1(4-4T_1^3+4T_1^4+4x_1y_1+4T_1^2(1+x_1y_1)-T_1(4+x_1y_1))}{4T_1^3}$$

```
In[9]:= Z5561 = tR6,1 tR2,7 tR8,12 tR3,9 tR10,4 tC11 tC5;
        Do[Z5561 = Z5561 // tm1,j→1,{j,2,12}];
        Coefficient[PowerExpand[Z5561[[3]] // Simplify], ϵ, 1]
```

$$\text{Out[9]}= -a_1^2T_1+\frac{a_1(-1+2T_1-x_1y_1+T_1^3(1+x_1y_1)-2T_1^2(2+x_1y_1))}{T_1}$$
$$-\frac{x_1y_1(4-4T_1^3+4T_1^4+4x_1y_1+4T_1^2(3+x_1y_1)-T_1(4+x_1y_1))}{4T_1^2}$$

5_{12} and 5_{593}:

In[10]:=
```
Z512 = tR1,6 tR7,2 tR11,5 tR4,10 tR9,13 tC3 tC12 tC8 tC14;
Do[Z512 = Z512 // tm1,j→1,{j,2,14}];
Coefficient[PowerExpand[Z512[[3]] // Simplify], ϵ, 1]
```

Out[10]=
$$\frac{1}{4T_1^5(1-T_1+T_1^2-T_1^3+T_1^4)^3}(-4a_1(2+5a_1)T_1^{18}-4(3+20a_1)T_1^7x_1y_1-120a_1T_1^9x_1y_1$$
$$-19x_1^2y_1^2+6T_1x_1^2y_1^2-32T_1^2x_1^2y_1^2+18T_1^3x_1^2y_1^2-39T_1^4x_1^2y_1^2+T_1^8x_1y_1(-4+96a_1-35x_1y_1)$$
$$+4T_1^6x_1y_1(1+12a_1-11x_1y_1)+2T_1^5x_1y_1(-8-20a_1+x_1y_1)+T_1^{11}(4+40a_1^2-20x_1y_1$$
$$-6x_1^2y_1^2+a_1(60-84x_1y_1))+2T_1^{13}(-8+40a_1^2-24x_1y_1-3x_1^2y_1^2+a_1(44-24x_1y_1))$$
$$-4T_1^{10}(2+5a_1^2+2x_1y_1+7x_1^2y_1^2+a_1(9-17x_1y_1))+4T_1^{17}(-1+10a_1^2-2x_1y_1$$
$$+a_1(5-3x_1y_1))-4T_1^{14}(-6+25a_1^2-11x_1y_1+2x_1^2y_1^2-6a_1(-4+x_1y_1))$$
$$+T_1^{16}(16-60a_1^2+20x_1y_1-3x_1^2y_1^2+12a_1(-3+x_1y_1))+T_1^{12}(8-60a_1^2+24x_1y_1-15x_1^2y_1^2$$
$$+a_1(-76+52x_1y_1))+T_1^{15}(80a_1^2+a_1(60-36x_1y_1)-2(12+18x_1y_1+x_1^2y_1^2)))$$

In[11]:=
```
Do[Z512op = Z512 // tS1, 1];
Coefficient[PowerExpand[Z512op[[3]] // Simplify], ϵ, 1]
```

Out[11]=
$$\frac{1}{4T_1^6(1-T_1+T_1^2-T_1^3+T_1^4)^3}(-20a_1^2T_1^{18}+4(1-20a_1)T_1^7x_1y_1-24(-1+5a_1)T_1^9x_1y_1$$
$$-19x_1^2y_1^2+6T_1x_1^2y_1^2-32T_1^2x_1^2y_1^2+18T_1^3x_1^2y_1^2-39T_1^4x_1^2y_1^2+2T_1^5x_1y_1(-4-20a_1+x_1y_1)$$
$$-4T_1^6x_1y_1(1-12a_1+11x_1y_1)+T_1^{11}(28+40a_1^2+28x_1y_1-6x_1^2y_1^2+a_1(44-84x_1y_1))$$
$$-4T_1^{10}(4+5a_1^2+8x_1y_1+7x_1^2y_1^2+a_1(7-17x_1y_1))-4T_1^{14}(6+25a_1^2+5x_1y_1+2x_1^2y_1^2$$
$$+a_1(14-6x_1y_1))+4T_1^{17}(1+10a_1^2+2x_1y_1+a_1(1-3x_1y_1))-T_1^{12}(32+60a_1^2+32x_1y_1$$
$$+15x_1^2y_1^2-52a_1(-1+x_1y_1))-T_1^{16}(8+60a_1^2+12x_1y_1+3x_1^2y_1^2-12a_1(-1+x_1y_1))$$
$$+T_1^{13}(32+80a_1^2+24x_1y_1-6x_1^2y_1^2-8a_1(-7+6x_1y_1))+T_1^8x_1y_1(96a_1-5(4+7x_1y_1))$$
$$+2T_1^{15}(8+40a_1^2+10x_1y_1-x_1^2y_1^2-2a_1(-7+9x_1y_1)))$$

In[12]:=
```
Z5593 = tR1,6 tR7,2 tR8,12 tR3,9 tR10,4 tC11 tC5;
Do[Z5593 = Z5593 // tm1,j→1,{j,2,12}];
Coefficient[PowerExpand[Z5593[[3]] // Simplify], ϵ, 1]
```

Out[12]=
$$\frac{1}{4T_1^5(1-T_1+T_1^2-T_1^3+T_1^4)^3}(-4a_1(2+5a_1)T_1^{18}-4(3+20a_1)T_1^7x_1y_1-120a_1T_1^9x_1y_1$$
$$-19x_1^2y_1^2+6T_1x_1^2y_1^2-32T_1^2x_1^2y_1^2+18T_1^3x_1^2y_1^2-39T_1^4x_1^2y_1^2+T_1^8x_1y_1(-4+96a_1-35x_1y_1)$$
$$+4T_1^6x_1y_1(1+12a_1-11x_1y_1)+2T_1^5x_1y_1(-8-20a_1+x_1y_1)+T_1^{11}(28+40a_1^2+4x_1y_1$$
$$-6x_1^2y_1^2+a_1(60-84x_1y_1))-T_1^{12}(32+60a_1^2+16x_1y_1+15x_1^2y_1^2+a_1(76-52x_1y_1))$$
$$+T_1^{13}(32+80a_1^2-6x_1^2y_1^2+a_1(88-48x_1y_1))-4T_1^{10}(4+5a_1^2+4x_1y_1+7x_1^2y_1^2$$
$$+a_1(9-17x_1y_1))+4T_1^{17}(1+10a_1^2+a_1(5-3x_1y_1))-4T_1^{14}(6+25a_1^2+x_1y_1+2x_1^2y_1^2$$
$$-6a_1(-4+x_1y_1))-T_1^{16}(8+60a_1^2+4x_1y_1+3x_1^2y_1^2-12a_1(-3+x_1y_1))$$
$$+2T_1^{15}(8+40a_1^2+2x_1y_1-x_1^2y_1^2-6a_1(-5+3x_1y_1)))$$

It may be non-obvious from this output that $Z_{\mathbb{D}}(5_{12}) \neq Z_{\mathbb{D}}(5_{593})$, so we let Mathematica verify this below:

In[13]:=
```
PowerExpand[Simplify[Z5593[[3]]-Z512[[3]]]]
```

Out[13]=
$$\frac{2T_1^5(-1+2T_1-2T_1^2+T_1^3)(1+x_1y_1)\epsilon}{(1-T_1+T_1^2-T_1^3+T_1^4)^2}+O[\epsilon]^2$$

References

1. Bar-Natan, D., van der Veen, R.: Perturbed gaussian generating functions for universal knot invariants. arXiv preprint arXiv:2109.02057 (2021)
2. Cox, M.A., Hughes, T.S., Ellis-Monaghan, J.A., Mondanaro, K.R.: Hydrocarbon links in an octet truss. J. Math. Chem. **43**(2), 874–891 (2008)

3. Dorier, J., Goundaroulis, D., Benedetti, F., Stasiak, A.: Knoto-id: a tool to study the entanglement of open protein chains using the concept of knotoids. Bioinformatics **34**(19), 3402–3404 (2018)
4. Erdman, J.M.: A problem text in advanced calculus. Portland State University (2005)
5. Everaers, R., Kremer, K.: Topological interactions in model polymer networks. Phys. Rev. E **53**(1), R37 (1996)
6. Gabrovšek, B.: An invariant for colored bonded knots. Stud. Appl. Math. **146**(3), 586–604 (2021)
7. Goundaroulis, D., Dorier, J., Stasiak, A.: A systematic classification of knotoids on the plane and on the sphere. arXiv preprint arXiv:1902.07277 (2019)
8. Goundaroulis, D., Gügümcü, N., Lambropoulou, S., Dorier, J., Stasiak, A., Kauffman, L.: Topological models for open-knotted protein chains using the concepts of knotoids and bonded knotoids. Polymers **9**(9), 444 (2017)
9. Gügümcü, N., Kauffman, L.H.: New invariants of knotoids. Eur. J. Comb. **65**:186–229 (2017)
10. Habiro, K.: Bottom tangles and universal invariants. Algebraic Geom. Topol. **6**(3), 1113–1214 (2006)
11. Jamroz, M., Niemyska, W., Rawdon, E.J., Stasiak, A., Millett, K.C., Sułkowski, P., Sulkowska, J.I.: Knotprot: a database of proteins with knots and slipknots. Nucleic Acids Res. **43**(D1):D306–D314 (2015)
12. Kauffman, L.H.: Rotational virtual knots and quantum link invariants. J. Knot Theory Ramif. **24**(13):1541008 (2015)
13. Kodokostas, D., Lambropoulou, S.: Rail knotoids. J. Knot Theory Ramif. **28**(13), 1940019 (2019)
14. Mansfield, M.L.: Are there knots in proteins? Nat. Struct. Biol. **1**(4):213–214 (1994)
15. Moltmaker, W.: Framed knotoids and their quantum invariants. Commun. Math. Phys. 1–27 (2022)
16. Morse, A., Adkisson, W., Greene, J., Perry, D., Smith, B., Ellis-Monaghan, J., Pangborn, G.: DNA origami and unknotted a-trails in torus graphs. J. Knot Theory Ramif. **29**(07), 2050041 (2020)
17. Ohtsuki, T.: Quantum Invariants: A Study of Knots, 3-Manifolds, and Their Sets, volume 29. World Scientific (2002)
18. Panagiotou, E., Kauffman, L.H.: Knot polynomials of open and closed curves. Proc. R. Soc. A **476**(2240):20200124 (2020)
19. Panagiotou, E., Kauffman, L.H.: Vassiliev measures of complexity for open and closed curves in 3-space. arXiv preprint arXiv:2104.12275 (2021)
20. Sułkowska, J.I., Rawdon, E.J., Millett, K.C., Onuchic, J.N., Stasiak, A.: Conservation of complex knotting and slipknotting patterns in proteins. Proc. Natl. Acad. Sci. 109(26):E1715–E1723 (2012)
21. Turaev, V.: Knotoids. Osaka J. Math. **49**(1), 195–223 (2012)
22. Wolfram Research, Inc. Mathematica, Version 13.1. Champaign, IL (2022)

Communicated by C. Schweigert